

WDM Soliton Transmission System Using Dispersion Slope Compensators

Shy-Chaung Lin, Sien Chi, and Jeng-Cherng Dung

Abstract—A new scheme of dispersion slope compensator by writing Bragg gratings at different positions in a dispersion compensation fiber is proposed for the wavelength division multiplexing soliton transmission system. This scheme can compensate in-line for the accumulated dispersion of each channel and suppress the dispersive waves which are caused by the incomplete filtering of the signals of the neighboring channels by using Fabry–Perot or Butterworth filters and the different propagating paths of the signals of the different channels in the dispersion slope compensator.

Index Terms—Dispersion slope compensation, fiber Bragg grating, optical solitons.

THE wavelength-division-multiplexing (WDM) soliton transmission system is limited by the timing jitter caused by the soliton interactions, the amplifier spontaneous emission (ASE) noise (Gordon–Haus effect), and the unsymmetrical collisions between different channels. By using the dispersion compensation fibers (DCF's) [1]–[3] or chirped fiber Bragg gratings (FBG's) [4], the dispersion compensation techniques are suggested to compensate for the group-velocity dispersion and improve the system performance. Since the wavelength dependence of the dispersion in the fiber, the signals of different channels suffer different dispersion, a single bare DCF cannot compensate for the dispersion of all channels in an optical WDM transmission system. To overcome this problem of dispersion slope, a quadratically chirped fiber Bragg grating [5] and dispersion slope compensator-A (DSC-A) [3] as shown in Fig. 1 was proposed, the DSC-A that first divided the WDM signal channels into different paths by the optical fiber coupler and each channel was selected by an optical bandpass filter placed on each path and then were recombined by the optical fiber coupler following the individual DCF's. Because there are two optical fiber couplers for signal division and combining in this scheme, 3-dB loss for either division or combining is unavoidable. These losses increase with the number of channels.

In the DSC, some fractional energy of the signal of a channel appears in the neighboring paths because of the incomplete filtering process due to the finite spectral side-level of the optical bandpass filter. This fractional pulse propagates in a different path from the principal pulse. After the DSC the fractional pulses lead or lag behind the principal pulses

Manuscript received July 28, 1998; revised September 22, 1998. This work was supported by the National Science Council of the Republic of China under Contract NSC 87-2215-E-009-014.

The authors are with the Institute of Electro-Optical Engineering, National Chiao Tung University, Hsinchu, Taiwan 30050, R.O.C.

Publisher Item Identifier S 1041-1135(99)00336-5.

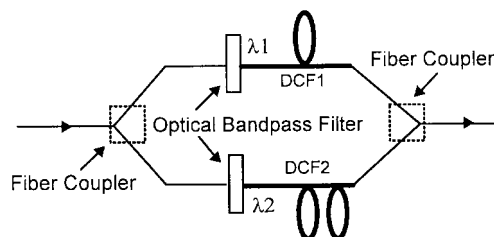


Fig. 1. The dispersion slope compensator-A (DSC-A), used by Suzuki *et al.*

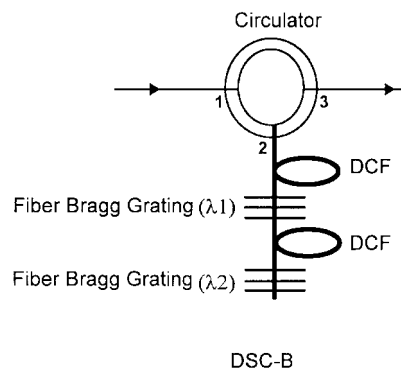


Fig. 2. The dispersion slope compensator-B (DSC-B), a new scheme of the dispersion slope compensator.

and become the dispersive waves. Such dispersive waves are accumulated along the transmission distance and degrade the transmission system. In this letter, we propose a new scheme of DSC-B as shown in Fig. 2. The FBG's with different central frequencies, playing the role of bandpass filters, can be written at the different positions of a DCF to reflect the signals of different channels. Therefore, the signals of different channels suffer different dispersion due to their different propagating distances in the DCF. The major merits of our scheme are that the accumulated dispersion of different channels can be in-line compensated, i.e., there are no division and combining loss, and the total length of DCF's can be greatly reduced. We will show that the dispersive waves are serious when the Fabry–Perot filters (FPF) are used. The fiber Bragg grating can be properly designed to have a rectangular-like spectrum profile to avoid incomplete filtering. Therefore, by proper design, the allowed transmission distance by using the DSC-B is larger than those by using the FPF or Butterworth filter (BWF) in the DSC-A.

The wave equation describing a soliton transmission in a single-mode fiber can be described by the modified nonlinear

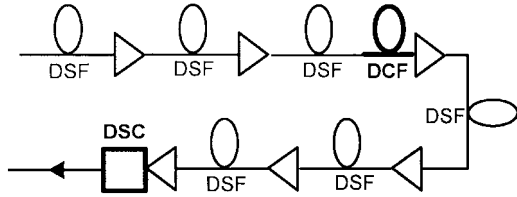


Fig. 3. The schematic diagram of a unit cell in a WDM soliton transmission system with dispersion slope compensation.

Schrödinger equation

$$i \frac{\partial U}{\partial z} - \frac{1}{2} \beta_2 \frac{\partial^2 U}{\partial \tau^2} - i \frac{1}{6} \beta_3 \frac{\partial^3 U}{\partial \tau^3} + n_2 \beta_0 |U|^2 U - C_r U \frac{\partial}{\partial \tau} |U|^2 = \frac{i}{2} \alpha U \quad (1)$$

where $\tau = t - \beta_1 z$ and β_1 is the reciprocal group velocity, β_2 and β_3 represent the second-order and third-order dispersion of the fiber, respectively, U is the slowly varying amplitude, n_2 is the Kerr coefficient, C_r is the slope of Raman gain profile, and α is the loss coefficient of the fiber. For the numerical simulation, the coefficients in (1) are taken as $\beta_2 = 0.14 \text{ ps}^2/\text{km}$, $n_2 = 2.6 \times 10^{-20} \text{ m}^2/\text{W}$, $C_r = 3.8 \times 10^{-16} \text{ (ps}\cdot\text{m)/W}$, and $\alpha = 0.22 \text{ dB/km}$. According to the experiment of Suzuki *et al.* [3], the schematic diagram of a unit cell in a WDM soliton transmission system with dispersion slope compensation is shown in Fig. 3. The amplifier spacing is 35 km. The second-order dispersion of DCF's is $137 \text{ ps}^2/\text{km}$ [6]. A single bare DCF was placed at $z = 105 \text{ km}$, then the DSC was placed at $z = 210 \text{ km}$. The length of the single DCF was 1.0144 km. The signal central wavelengths $\lambda_1 = 1557.2 \text{ nm}$ and $\lambda_2 = 1560 \text{ nm}$, the second-order dispersions were -0.88 and $-1.188 \text{ ps}^2/\text{km}$ for λ_1 and λ_2 , respectively. The lengths of DCF's in the DSC-A are 0.28266 and 0.7582 km for DCF1 and DCF2, respectively. Therefore, the path-average second-order dispersion was $-0.04 \text{ ps}^2/\text{km}$ for each channel. We numerically model the experiment of Suzuki *et al.* by using the dispersion slope compensator-A (DSC-A) as shown in Fig. 1. The transfer function $H(\omega)$ of the optical bandpass filters in DSC-A are given as $H(\omega)_{\text{FPF}} = (1 - S)^{-1}$ and $H(\omega)_{\text{BWF}} = (1 + S^2 - \sqrt{2}S)^{-1}$, where $S = i2(\omega - \omega_j)/B$, ω_j is the central frequency, $j = 1, 2$, $B = 1.152 \text{ nm}$ is the filter bandwidth.

The reflectivity of a FBG can be calculated from the coupled-mode equations

$$\frac{dA^+}{dZ} = \kappa(z) \exp \left[-i \int_0^z B(z') dz' \right] A^- \quad (2a)$$

$$\frac{dA^-}{dZ} = \kappa(z) \exp \left[i \int_0^z B(z') dz' \right] A^+ \quad (2b)$$

where A^+ and A^- are the amplitude of the forward and backward propagating modes along the z direction. $\kappa(z) = \kappa_0 \exp(-30z^2/L^2)$ is the coupling coefficient and varies along the grating, where L is the length and κ_0 is the maximum coupling coefficient at central position for the FBG. $B(z) = 2\beta_j - 2\pi/\Lambda_j$, $j = 1, 2$ represents the phase mismatch of the grating and β_j is the propagation constant of the carrier wave for each channel, $\Lambda_j = \lambda_j \bar{n}/2$ is the grating period, λ_j is the

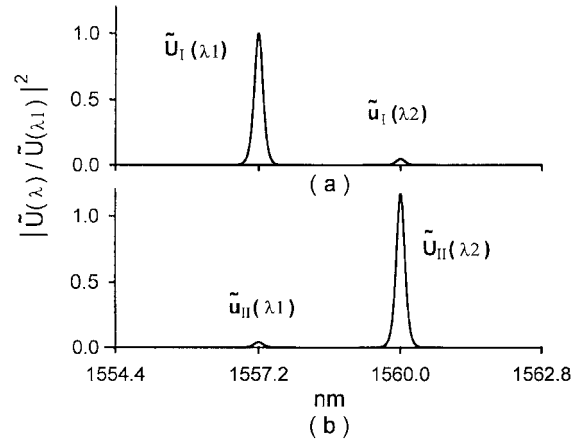


Fig. 4. The normalized spectra of the WDM signals after the FPF in (a) path-I and (b) path-II, respectively.

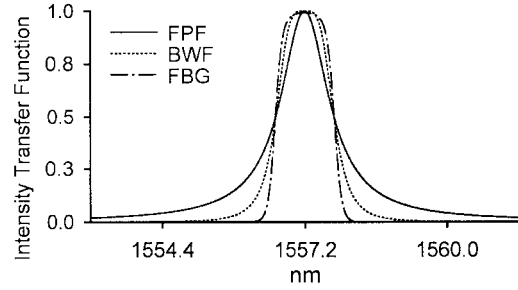


Fig. 5. The intensity transfer function for the FPF, BWF, and FBG filter, respectively.

central wavelength of carrier waves and \bar{n} is the mode index. The parameters of the FBG are chosen as $\kappa_0 L = 9.4$, $L = 4.4 \text{ mm}$, and the bandwidth of the FBG is 1.152 nm. In the DSC-B shown in Fig. 2, the signal λ_j propagates from $Z_{\text{DCF}} = 0$ to $Z_{\text{DCF}} = Z_j$, where Z_j indicates the position of FBG of λ_j , then the signal λ_j is reflected and propagates from $Z_{\text{DCF}} = Z_j$ to $Z_{\text{DCF}} = 0$, thus the effective length of DCF for the signal λ_j is $2Z_j$. The FBG's of Fig. 2 are written at positions $Z_1 = 0.14133 \text{ km}$ and $Z_2 = 0.3791 \text{ km}$ for λ_1 and λ_2 , respectively.

To show the dispersive waves, we use the FPF as the optical bandpass filter in the DSC-A. Fig. 4(a) and (b) show the normalized spectra of the WDM signals after the optical bandpass filters in path-I and path-II, respectively. In path-I, there are the principal pulse of λ_1 and the fractional pulse of λ_2 which is caused by incomplete filtering due to finite spectral side-level of the optical bandpass filter 1. In path-II, there are the principal pulse of λ_2 and the fractional pulse of λ_1 which is caused by incomplete filtering due to finite spectral side-level of the optical bandpass filter 2. The fractional pulse of λ_1 , propagating in path-II with a longer DCF, has a time delay with respect to the principal pulse of λ_1 in the path-I. Hence the fractional pulse of λ_1 through path-II is separated from the principal pulse of λ_1 through path-I after the DSC. The same phenomenon happens in λ_2 channel.

The incident soliton pulse with linear frequency chirp is assumed to be of the form $U(z = 0, \tau) = \eta_0 \text{sech}(\tau) \exp(-iC_0 \tau^2/2)$, where η_0 is the initial pulse

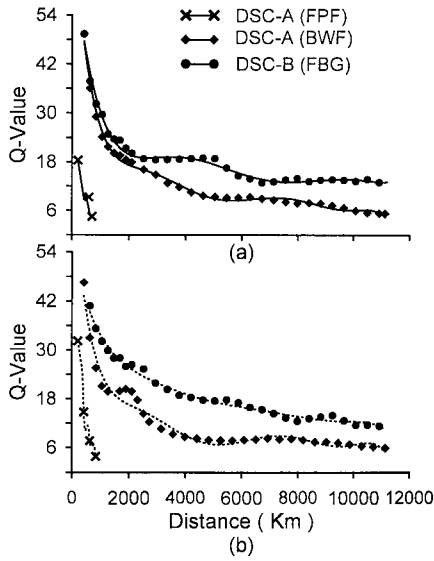


Fig. 6. The Q -value of (a) λ_1 - and (b) λ_2 -channels in the WDM transmission system with dispersion slope compensation versus propagation distance by using the different DSC's. The DSC-A(FPF), DSC-A(BWF), and DSC-B(FBG) indicate the DSC-A with FPF, BWF, and DSC-B with FBG, respectively.

amplitude and $C_o = 0.5$ represents the pre-chirping parameter. The initial pulsewidth of signal $\tau_{FWHM} = 1.763\tau = 12.5$ ps, the bit rate is 20 Gb/s for the single channel, the average powers are -0.01087 and 0.6632 dBm for λ_1 and λ_2 , respectively. Fig. 5 shows the intensity transfer function of the different optical bandpass filters. It can be seen that the FPF has the most serious spectral side-level and the FBG filter has the least serious spectral side-level. For the transmission system shown in Fig. 3, we simulate the soliton transmission by using the FPF and the BWF in the DSC-A, and by using the FBG in the DSC-B. We use the 512 pseudorandom bits for the simulations. With the different DSC's, Fig. 6(a) and (b) show the Q -value versus propagation distance for λ_1 and

λ_2 , respectively. A 10^{-9} bit-error rate (BER) corresponds to $Q = 6$. For a 10^{-9} BER, the allowed transmission distances are 630 and 10080 km by using the FPF and the BWF in the DSC-A, respectively. By using the DSC-B, the allowed transmission distance is well beyond 10080 km. If the extra division and combining losses in DSC-A are considered, the performance of DSC-B is much better than DSC-A.

In conclusion, we have proposed a new scheme of dispersion slope compensator by writing the fiber Bragg gratings in a dispersion compensation fiber for the WDM soliton transmission system, however, this novel proposal can also apply to multichannel linear WDM transmission system. With this new dispersion slope compensator, the accumulated dispersion of signals of different channels can be compensated in-line and there is no division loss. The dispersive wave, which is caused by incomplete filtering due to the finite spectral side-level of an optical bandpass filter and the different propagating paths of different channels, is also suppressed by the FBG in the proposed dispersion slope compensator.

REFERENCES

- [1] M. Suzuki, I. Morita, N. Edagawa, S. Yamamoto, H. Taga, and S. Akiba, "Reduction of Gordon-Haus timing jitter by periodic dispersion compensation in soliton transmission," *Electron Lett.*, vol. 31, pp. 2027–2029, 1995.
- [2] N. J. Smith, F.M. Knox, N. J. Doran, K. J. Blow, and I. Bennion, "Enhanced power solitons in optical fibers with periodic dispersion management," *Electron Lett.*, vol. 32, pp. 54–55, 1996.
- [3] M. Suzuki, I. Morita, N. Edagawa, S. Yamamoto, and S. Akiba, "20 Gbits/s-based soliton WDM transmission over transoceanic distances using periodic compensation of dispersion and its slope," *Electron Lett.*, vol. 33, pp. 691–692, 1997.
- [4] S. Chi, S. C. Lin, and J. C. Dung, "Reduction of soliton interactions and timing jitters by chirped fiber Bragg grating filters," *IEEE Photon. Technol. Lett.*, vol. 9, pp. 1643–1645, 1997.
- [5] J. A. R. Williams, L. A. Everall, I. Bennion, and N. J. Doran, "Fiber Bragg grating fabrication for dispersion slope compensation," *IEEE Photon. Technol. Lett.*, vol. 8, pp. 1187–1189, 1996.
- [6] A. J. Antos and D. K. Smith, "Design and characterization of dispersion compensating fiber based on the mode," *J. Lightwave Technol.*, vol. 12, pp. 1739–1745, 1994.